


## Article

# Oxygen Plasma Improved Shear Strength of Bonding between Zirconia and Composite Resin

Min Yan <sup>1,2</sup>, Chun-Chuan Yang <sup>1,3</sup>, Yi-Hsuan Chen <sup>1</sup> and Shinn-Jyh Ding <sup>1,2,\*</sup> 

<sup>1</sup> Institute of Oral Sciences, Chung Shan Medical University, Taichung 402, Taiwan; yan@csmu.edu.tw (M.Y.); ycc@ms.szmc.edu.tw (C.-C.Y.); foryou052141@gmail.com (Y.-H.C.)

<sup>2</sup> Department of Dentistry, Chung Shan Medical University Hospital, Taichung 402, Taiwan

<sup>3</sup> Department of Dental Technology, Shu Zen Junior College of Medicine and Management, Kaohsiung 82144, Taiwan

\* Correspondence: sjding@csmu.edu.tw; Tel.: +886-4-24718668 (ext. 55529); Fax: +886-4-24759065

Received: 13 June 2020; Accepted: 29 June 2020; Published: 30 June 2020



**Abstract:** Improving the strength of the bonding of zirconia to composite resins remains a challenge in dental restorations. The purpose of this study was to evaluate the shear strength of the bonding of zirconia to composite resins, thereby verifying the hypothesis that as the power of the non-thermal oxygen plasma increases, the bonding strength of the plasma-treated zirconia is increased. The effects of the oxygen plasma power (100, 200, and 400 W) on the surface structure, chemical composition, and hydrophilicity of the zirconia and the strength of the bonding between zirconia and composite resin were investigated. As a result, after different plasma power treatments, the surface structure and phase composition of zirconia were not different from those of zirconia without treatment. However, the oxygen plasma treatment not only reduced carbon adsorption but also greatly increased the hydrophilicity of the zirconia surface. More importantly, the strength of the bonding between the plasma-treated zirconia and composite resin was significantly higher than that in the corresponding control group without plasma treatment. Regardless of whether the zirconia was pristine or sandblasted, the higher the plasma power, the greater the bond strength obtained. The conclusion is that the oxygen plasma treatment of zirconia can effectively improve the strength of the bonding between the zirconia and composite resin without damaging the microstructure and phase composition of the zirconia.

**Keywords:** zirconia; composite resin; oxygen plasma; shear bond strength

## 1. Introduction

General, dental restoration materials can be divided into metal, ceramic, and polymer resin materials. Considering the complexity of the oral environment, the restoration materials should exhibit good biocompatibility, extraordinary mechanical strength, high durability, and good aesthetics [1]. Despite the excellent mechanical strength of metals, dental metal allergy, gingival discoloration, and corrosion can still compromise the effectiveness and safety of metallic dental restorations [2–4]. Ceramics possess better chemical stability and biocompatibility, as well as superior compressive strength and hardness. However, the inherent brittleness of ceramics remains a major problem, which can increase the occurrence of unexpected fractures of dental restorations. Among dental ceramics, zirconia ceramics have outstanding bending strength and fracture toughness. By using computer-aided design/computer-aided manufacturing (CAD/CAM), the zirconia ceramic bulk can be shaped into dental cores, crowns, bridges, and frameworks for the bridges [5,6]. Composite resins are capable of being used for constructing dental restorations and offer distinguished properties and successful colour matching for adjacent teeth, with a facile preparation procedure. For example, they can be directly

employed for clinical operative dentistry by serving as filling materials. In addition, composite resins are also indirectly used for dental technologies to manufacture dental inlays, onlays, veneers, crown and bridge restorations, resin-veneered metallic crown and bridge restorations, and implant-supported restorations, and for the intraoral repair of chipped veneering porcelain [7]. The indirect composite resins are promising alternatives as veneering materials for zirconia ceramic frameworks due to their plasticity, viscoelasticity, creep, and recovery characteristics [8,9].

The strength of the bonding between different materials plays a vital role in determining the durability and service life of dental restorations. However, the strength of the bonding between the resin material and the substrate is usually low [10–15]. Many attempts have been made to enhance the bond strength. Not surprisingly, surface roughening treatments originating from increasing the surface roughness and surface area have been developed to improve this issue [11,15–19]. For example, the commonly used air-abrasion technique not only effectively improves the bonding strength of luting cements but also effectively enhances the strength of zirconia and veneering porcelain [16]. However, it may introduce surface damage, defects, and cracks on roughened zirconia, as well as internal stress caused by tetragonal-monolithic (t-m) phase transformation [19–24], which—in turn—can compromise the mechanical properties of zirconia. Besides, chemical surface modification techniques such as acid etching, primer spraying, silane coupling, and silica coating are also considered as promising methods to enhance bond strength. This is because the chemical modification simultaneously increases the surface roughness of the zirconia substrate without affecting its phase composition and provides surface chemistry suitable for promoting the formation of covalent bonds between the resin and the substrate [14,25–27]. However, it is noteworthy that acid etching using HF is dangerous and highly corrosive [11,14,25]. Moreover, chemical treatment requires complicated operational methods or the handling of highly toxic and hazardous substances, and is considered impractical in ordinary dental laboratories [25]. Thus, it is of great importance to develop alternative methods for effectively improving the strength of the bonding of zirconia to resin.

Plasma is an ionized gas comprised of electrons, ions, and free radicals. This is achieved by heating the gas to cause the dissociation of molecular bonds and subsequent ionization of free atoms [28]. Common plasma gases are oxygen, argon, nitrogen, or hydrogen. The applications of plasma technology are diverse, including cleaning, physical etching, deposition, and the surface modification of a substrate. It is well-documented that plasma treatments can remarkably alter the surface chemical properties of zirconia substrates [29]. Therefore, plasma treatment is used in the application of ceramic surface modification in order to activate the inert surface without causing changes in the microstructures, crystal phase, and mechanical properties [30]. In addition, plasma treatment can enhance the surface energy and wettability of the substrate [29,31,32], thereby improving the bond strength of the resin-based adhesive on the ceramic surface [33–37]. However, there is no evidence to verify the effect of oxygen plasma power on the bonding performance of zirconia. To this end, we tested the hypothesis that the shear bond strength increases with an increase in oxygen plasma power.

## 2. Materials and Methods

### 2.1. Zirconia Preparation

Commercially available zirconia ceramics for a CAD/CAM system (Vita YZ-55 In-Ceram, VITA, Bad Säckingen, Germany) and dental indirect composite resins (Ceramage body A3B, Shofu Inc. Kyoto, Japan) were used as substrate materials and veneering resin, respectively. Accordingly, Table 1 gives a description of the experimental materials used.

**Table 1.** The experimental materials used in this study.

Material	Composition (%)	Lot. No.	Manufacturer
Vita YZ-55 In-Ceram	ZrO <sub>2</sub> : 91–94%; Y <sub>2</sub> O <sub>3</sub> : 4–6%; HfO <sub>2</sub> : 2–4%; Al <sub>2</sub> O <sub>3</sub> : < 0.1	29730	VITA, Germany
Ceraresin Bond I and II	Bond I: Ethanol, silane coupling agent, etc. Bond II: Acetone, 4-AET, UDMA, polymerization initiator, etc.	121926 101925	Shofu, Japan
Ceramage (body A3B)	UDMA, Urethane diacrylate, Zirconium silicate, colouring materials, etc.	051918	Shofu, Japan

Square specimens were fabricated from pre-sintered zirconia blanks with a dental model saw (G2 Concept, Schick dental Geräte, Schemmerhofen, Germany). The surface of each specimen was polished with grit 800 SiC sandpaper, ultrasonically cleaned in deionized water for 10 min, and then dried. The specimens were sintered from room temperature to 1530 °C at a heating rate of 17 °C/min, held at 1530 °C using a high-temperature speed sintering furnace (Mihm-Vogt, Stutensee-Blankenloch, Germany) for 2 h, and then cooled to room temperature according to the instructions of the manufacturers. The final dimensions of the specimens (10 mm in length, 5 mm in width, and 3 mm in thickness) were obtained.

## 2.2. Plasma Treatment

The sintered zirconia specimens were divided into 2 groups (Group C and Group SB). The control group (Group C) represented the pristine surface without sandblasting. The sandblasting group (Group SB) were exposed to 50 µm Al<sub>2</sub>O<sub>3</sub> powder (Korox; Bego, Bremen, Germany) under a blasting pressure of 0.3 MPa for 10 seconds from a distance of 10 mm. All specimens with and without sandblasting were washed by ultrasonic cleaning in acetone, alcohol, and distilled water for 5 min each and dried in a common oven (CDV-452; Chengsheng, Tainan, Taiwan) at 60 °C for 30 min. Regarding plasma treatment using a plasmochemical generator (Femto, Diener Electronic, Ebhausen, Germany), the specimens were placed in a chamber evacuated to a base pressure lower than 0.4 mbar and then backfilled with high-purity oxygen gas until the working pressure was 0.6 mbar. Source powers of 100, 200, and 400 W were used to generate plasma to process Group C for 1 min, corresponding to the sample code C1, C2, and C4 groups, respectively, and C0 was a specimen without plasma treatment. Similarly, Group SB was divided into four subgroups: SB0, SB1, SB2, and SB4.

## 2.3. Resin Binding to Zirconia

The bonding agents I and II (Ceraresin bond I and II), as primers of zirconia ceramics, were applied at a 0.1 mm thickness to the surface of each zirconia substrate for 10 seconds. Afterwards, according to the manufacturer's recommendations, the bond agent was cured with a light-curing machine (Labolight LV-III, GC, Tokyo, Japan) for 3 min. To obtain a constant specimen size, a square steel mould with a hole dimension of 4 × 4 × 2 mm<sup>3</sup> was fixed on the zirconia substrate. The light-curing micro-hybrid composite resin (Ceramage body resin A3B, Shofu, Japan) as a veneering layer was filled into the designed hole 3 times, and curing was performed for 40 seconds each time. The specimen was stored in deionized water at 37 °C for 24 h.

## 2.4. Morphology and Phase Analyses

The surface morphology of specimens exposed to different plasma treatments was observed by field-emission scanning electron microscopy (FESEM; JSM-7800F, JEOL, Tokyo, Japan) after sputter-coating the surfaces with gold. The interface between the zirconia and resin was also examined by FESEM. Phase analysis was performed using an X-ray diffractometer (XRD; MINIFLEX-II, Rigaku, Tokyo, Japan) with Cu-Kα radiation (1.54 Å) operated at 30 kV and 15 mA with a 2θ range between

25° and 65° at a scanning speed of 1°/min. The Zr and O element distribution on the treated surfaces was determined under an X-ray photoelectron spectroscopy system (XPS; ULVAC-PHI, PHI 5000 VersaProbe, Osaka, Japan).

### 2.5. Roughness and Contact Angle

A surface analyser (Surfcom 50A, Tokyo Seimitsu, Tokyo, Japan) was used to determine the surface roughness value (Ra) of each specimen at five measurement positions, with a traverse length of 2.4 mm and a cut-off length of 0.8 mm. Five specimens were measured in each experimental group. An optical contact angle measurement and contour analysis system (OCA-15 SCA20, Data-Physics Instruments, Filderstadt, Germany) was applied to measure the contact angle. Ten specimens were measured for each condition.

### 2.6. Shear Bond Strength

A universal testing machine (AG-1000E, Shimadzu, Kyoto, Japan) with a crosshead rate of 1.0 mm/min was employed for the shear bond test. A 1 mm-thick knife-edge blade was used to apply a vertical loading force until the failure of the bond between zirconia and the composite resin, according to ISO 11405 [38]. Ten specimens were measured for each condition. The shear bond strength of the specimens was calculated with the following formula:

$$\text{SBS} = F/A \quad (1)$$

where SBS = shear bond strength (MPa), F = load at fracture (N), and A = area (mm<sup>2</sup>).

After the shear bond strength test, the amount of composite resin remaining on the surface of the zirconia specimen surface was observed, to evaluate the fracture modes of the specimens.

### 2.7. Statistical Analysis

One-way analysis of variance (ANOVA) and the Tukey–Kramer comparison test were used for the statistical evaluation of shear bond strengths. The Kruskal–Wallis test and the non-parametric multiple comparison test were used to statistically evaluate the surface roughness and contact angles of the specimens to determine significant differences. All the tests were performed at a significance level of 0.05 and with a 60% statistical power (sample size = 10) using a software package (JMP14; SAS Institute Inc., Cary, NC, USA).

## 3. Results

### 3.1. Surface Morphology

The surface morphology of the zirconia specimens with sandblasting (Group SB) was remarkably different from that of those without sandblasting (Group C), as shown in Figure 1. Regardless of the plasma power used, Group C showed a uniform grain size of about 300 nm. By contrast, as expected, all the SB groups had a rough and irregular appearance that was not affected by the plasma power.

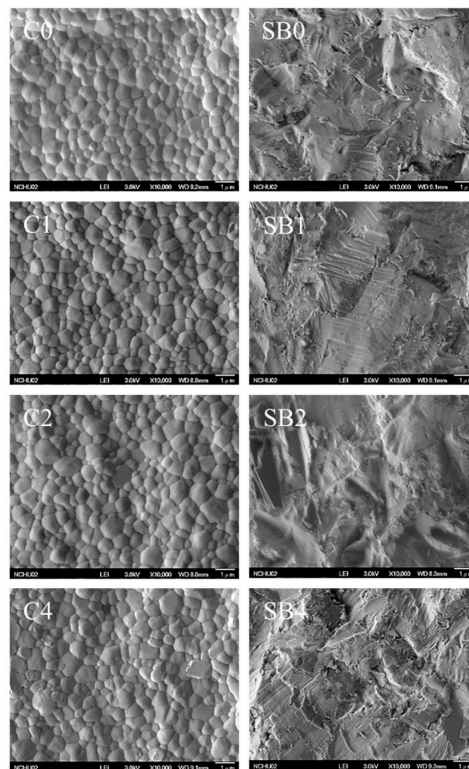


**Figure 1.** SEM images of the two zirconia surfaces before and after treatment with different plasma powers.

### 3.2. Phase Composition

Figure 2 shows the XRD patterns of different specimens before and after plasma treatment. The C0 specimen without sandblasting exhibited a well-crystallized tetragonal phase of the zirconia. The four characteristic peaks at  $2\theta = 30.27^\circ$ ,  $35.25^\circ$ ,  $50.37^\circ$ , and  $60.20^\circ$  were assigned to the (101), (110), (112), and (211) tetragonal phases, respectively (Figure 2a). In the case of the SB0 specimen, a small amount of monoclinic zirconia, as evidenced by a new characteristic peak at  $2\theta = 28.17^\circ$ , was observed (Figure 2b). Nevertheless, different oxygen plasma powers did not affect the peak intensity and position of the zirconia phase.

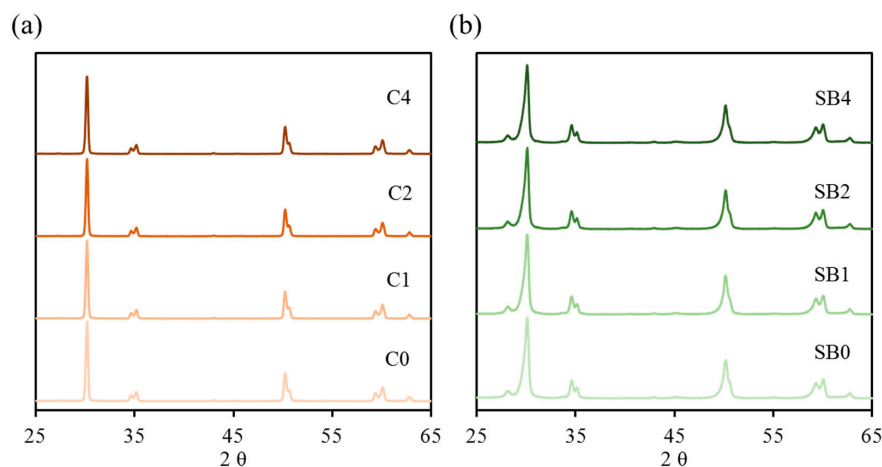


**Figure 2.** XRD patterns of (a) Group C and (b) Group SB before and after treatment with different plasma powers.

### 3.3. Chemical Composition

To further understand the effect of plasma treatment on the chemical composition of zirconia, XPS was used to characterize the surface chemical properties of Group SB. The characteristic peaks of C 1s, O 1s, Zr 3s, Zr 3p, and Zr 3d are shown in Figure 3a with a range of 100 to 600 eV. After calculating the C/O intensity ratio, the C/O ratio (0.29) of the 400 W-plasma-treated zirconia specimen (SB4) was lower than that of the SB0 control (0.34). The high-resolution photoelectron signal of Zr 3d is shown in Figure 3b, indicating that the binding energies of Zr 3d<sub>3/2</sub> and Zr 3d<sub>5/2</sub> were 183.4 and 181.0 eV, respectively, which clearly indicated the presence of fully oxidized zirconium in its Zr<sup>4+</sup> state, as expected in ZrO<sub>2</sub> [39]. It is worth noting that the intensity of Zr 3d on the plasma-treated surface appeared to be somewhat increased, possibly due to the refinement of the microstructure. Figure 3c shows the O 1s high-resolution signal at 529.2 eV. Compared with the SB0 group without plasma treatment, the oxygen plasma-treated specimens had higher intensity. The peak intensity of O 1s increased with the increase in plasma power. For example, that for the SB4 group was 21% higher than that for the SB0 control group.

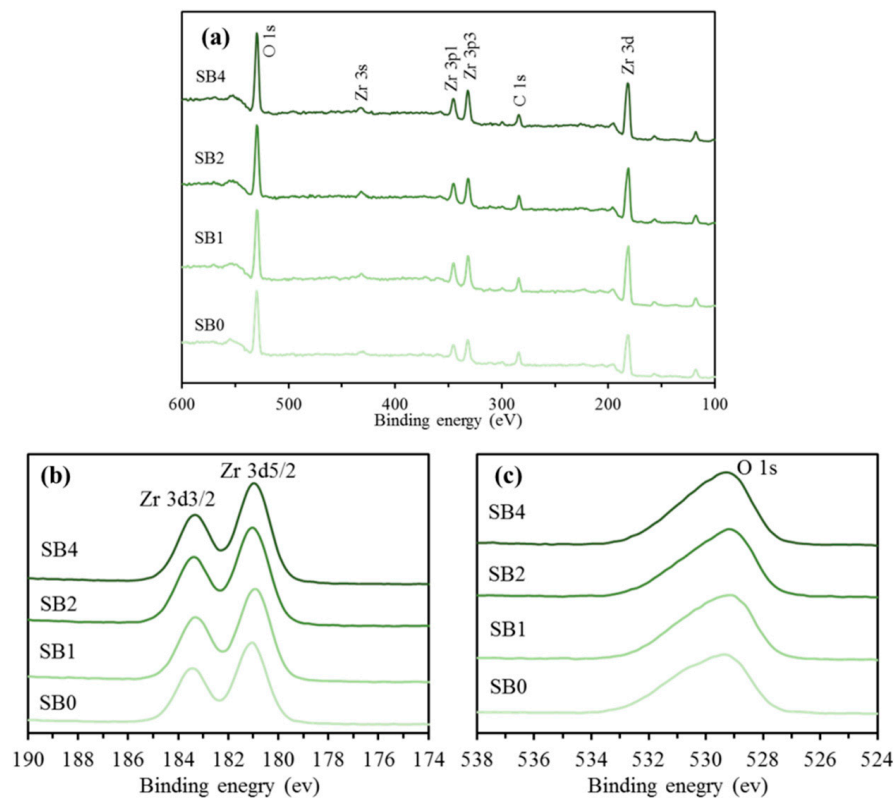


**Figure 3.** (a) XPS spectra of the Group SB specimen surfaces with different plasma treatments, and high-resolution XPS analyses of (b) Zr 3d and (c) O 1s.

### 3.4. Surface Roughness

The surface roughness (Ra) values of different specimens are shown in Figure 4. The statistical analysis of the Wilcoxon/Kruskal–Wallis tests illustrated that the Ra value (about 0.4  $\mu\text{m}$ ) of the Group SB specimens was significantly higher ( $p < 0.05$ ) than that (about 0.3  $\mu\text{m}$ ) of the Group C specimens. It can be clearly seen that regardless of whether the specimen was sandblasted or not, the plasma treatment will not change the roughness of the specimen surface.



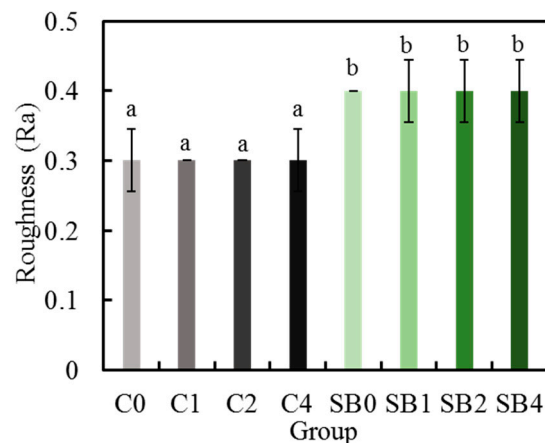


**Figure 4.** The surface roughness values of the zirconia before and after plasma treatment. The different letters “a” and “b” indicate significant differences ( $p < 0.05$ ) ( $n = 5$ ).

### 3.5. Contact Angle

The water contact angle can be used to check the surface hydrophilicity of the material. Figure 5 shows the images and contact angle values of the specimens in each group. Before the plasma treatment, the C0 and SB0 groups had the highest contact angle values, of  $68^\circ \pm 3^\circ$  and  $65^\circ \pm 4^\circ$ , of all the groups, respectively. However, plasma treatment caused a significantly ( $p < 0.05$ ) lower contact angle. For example, the contact angle values of SB1, SB2, and SB4 were  $28^\circ$ ,  $28^\circ$ , and  $25^\circ$ , respectively. Interestingly, there was no significant ( $p > 0.05$ ) difference between Group C and Group SB with the same plasma treatment condition.

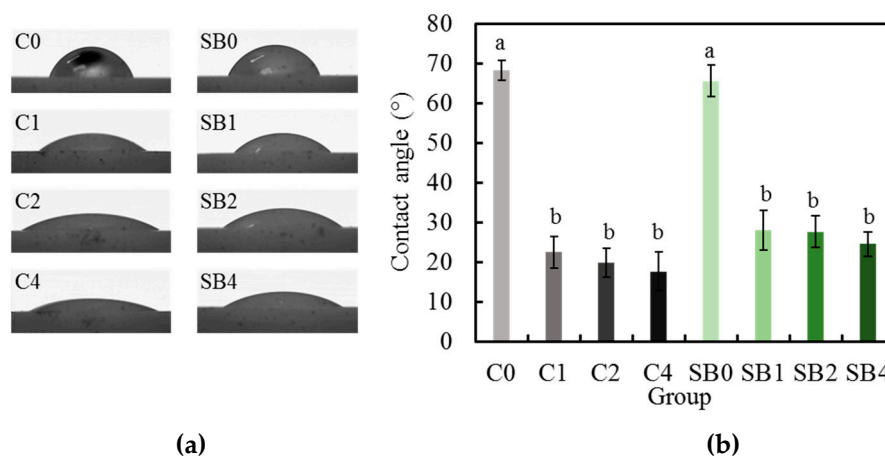


**Figure 5.** (a) Contact angle and images of water droplets on the different specimen surfaces with and without plasma treatments; (b) The different characters of “a” and “b” showed significant differences ( $p < 0.05$ ) ( $n = 10$ ).

### 3.6. Cross-Sectional Structure

The interfacial morphology of the specimens is shown in Figure 6. The SEM images indicated that the resin was well-attached to zirconia, except in the C0 group, with a gap at the interface. Furthermore, the ceramic–resin junctions in all the plasma-treated groups had no obvious structural defects or pores.

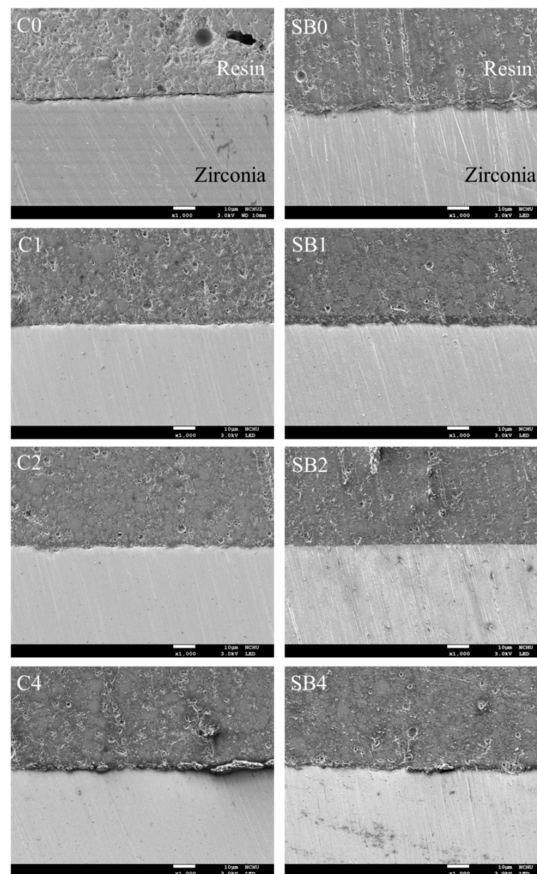


**Figure 6.** Cross-sectional SEM images of various plasma-treated zirconia bond to composite resin.

### 3.7. Shear Bond Strength

The shear bond strength of the specimens is shown in Figure 7. With the increase in plasma power, the shear bond strengths of Group C and Group SB increased significantly ( $p < 0.05$ ). It is worth noting that the SB4 group exhibited the highest bond strength, of  $6.1 \pm 0.8$  MPa, of all the test groups. In addition, under the same plasma power treatment, the bond strength value of the sandblasted specimens (Group SB) was significantly ( $p < 0.05$ ) higher than that of the corresponding non-sandblasted specimens (Group C).

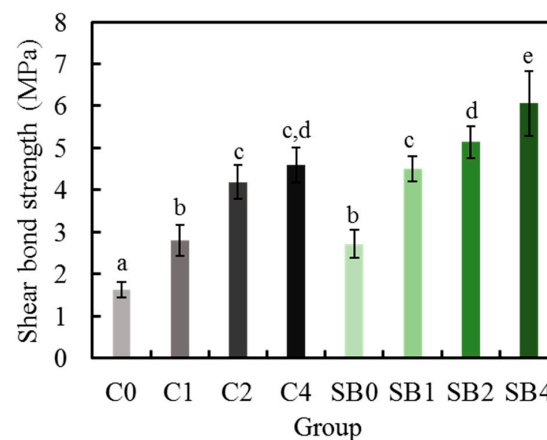


**Figure 7.** Shear strength of the bonding of the plasma-treated Y-TZP samples to resin. The different letters indicate significant differences ( $p < 0.05$ ) ( $n = 10$ ).



### 3.8. Fracture Analysis

Figure 8 shows fracture images of various specimens on the zirconia side after the shear bond tests. It is worth noting that the residual resin adhered to the plasma-treated surface, as indicated by the arrows, indicates a mixed mode of cohesive and interfacial fracture. Figure 9 shows the calculated fracture modes of the specimens. In the C0 and SB0 groups without plasma treatment, it can be seen from the photos that the veneering resin layers of all the specimens completely detached from the zirconia, which could be attributed to the occurrence of adhesive fractures (100%). For the plasma-treated group, the C1, C2, and C4 groups had mixed fractures of 10%, while the mixed fractures of the SB1, SB2, and SB4 groups increased to 40%. Not surprisingly, there was no cohesive fracture in any of experimental groups.

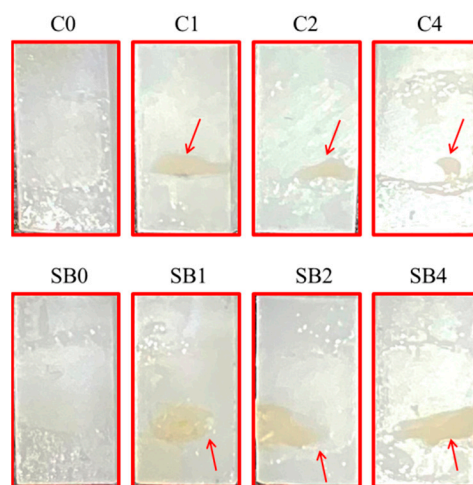


**Figure 8.** Fracture images of various Group C and Group SB specimens after shear bond testing. The arrow indicates the remained resin.

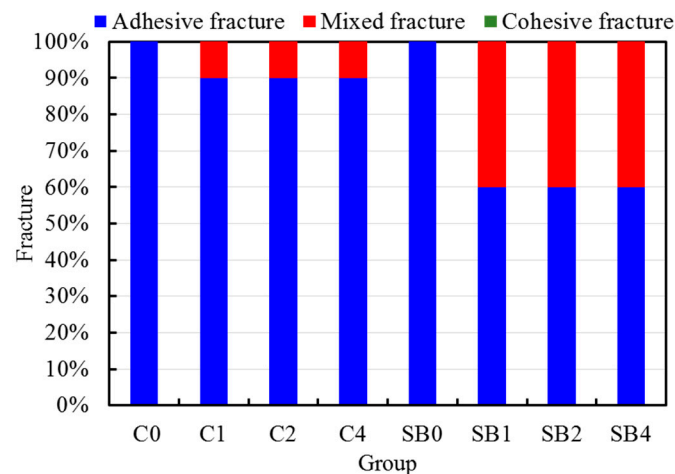


**Figure 9.** Fracture modes expressed as percentages of various zirconia–resin bonds after shear bond testing.

## 4. Discussion

In the present study, we attempted to evaluate the effect of oxygen plasma treatment with different powers on the efficiency of bonding between dental resin and zirconia with or without sandblasting. In addition, the morphology, chemical composition, and hydrophilicity of the plasma-treated zirconia were assessed. Compared with in the pristine specimens without sandblasting, the stress-induced

t-m phase transformation of zirconia was detected after sandblasting, which was consistent with the previous studies [19–24]. It is worth mentioning that the plasma treatment will not cause the phase transformation of zirconia, irrespective of whether or not sandblasting treatment is performed. In the study of Park et al. [35], an argon gas plasma at 10 W did not affect the zirconia phase. Similar to the findings, in the power range of 100–400 W, oxygen plasma treatment had no effect on the surface morphology and roughness of the zirconia.

It is well-recognized that a clean material surface is conducive to the efficient bonding between heterostructures, and plasma cleaning can effectively remove impurities and contaminants on the surfaces [40]. The excited particles generated in the plasma react with the surface layer of hydrocarbons and carbonate molecules, thereby oxidizing them to form  $H_2O$  and  $CO_2$ , which are desorbed from the surface and pumped away [32]. This might explain why a lower C/O ratio was found on the plasma-treated surface, as evidenced by the XPS results, and the higher intensity of elemental O with an increase in the plasma power. It is well documented that  $O_2$ -plasma treatment can introduce oxygen onto the surface of inert ceramic materials with a dense structure (e.g.,  $ZrO_2$ ) and subsequently facilitate the formation of reactive superoxide free radicals (R-O-O-), thereby inducing the alteration of the chemical composition of the ceramic surface [39]. This may be the main reason for the significant reduction in the contact angle after plasma treatment compared to that in the corresponding control groups without plasma treatment. In this study, the water contact angle of zirconia with or without sandblasting was about  $68^\circ$ , which was similar to that in a published report [38]. Regardless of whether sandblasting treatment was performed, the contact angle was less than  $30^\circ$ , showing good hydrophilicity. Zhao et al. [41] pointed out that as the surface of the material becomes more oxidized or gains more ionizable groups, hydrogen bonding with water becomes easier, and the water droplet can spread, leading to a reduction in the contact angle.

Our study utilized facile plasma treatment to enhance the strength of the bonding between zirconia and resin, and clarified the effect of plasma power on the bond strength. Before exploring the plasma effect, it can be clearly observed that the shear bond strength increased with increasing surface roughness, which is consistent with the literature [11,19]. Lung et al. [26] found that the improvement of the strength of the bonding of the resin cement to zirconia by sandblasting was due to micro-mechanical interlocking. After plasma treatment, the shear bond strength of zirconia without sandblasting bonded to resin (C1, C2, and C4) was in the range of 2.8 to 4.6 MPa, which was about two times higher than that (1.63 MPa) of the control group (C0), with statistical significance. In the case of the sandblasting groups, oxygen plasma treatment could also effectively improve the shear strength of the bonding between the zirconia and the composite resin. More importantly, the bond strength can increase with increasing plasma power. In short, regardless of whether sandblasting was conducted or not, plasma treatment was an important factor influencing the bond strength. Despite the mechanism not being fully unveiled, it is speculated that plasma treatment could incorporate polar oxygen-based functional groups on the surface of zirconia, resulting in elevated surface energy and wettability, subsequently facilitating the spreading of resins while they are in contact the plasma-treated surface [30,32,42], thereby enhancing the bond strength. Previous studies have shown that the strength of the bonding between zirconia and resin cement could be increased by conducting plasma treatment in an argon, helium, oxygen, or hydrogen-containing mixture gas atmosphere [33–36].

The fracture analysis was conducted by observing the amount of resin remaining on the zirconia specimens after the shear bond strength testing. The two C0 and SB0 control groups revealed adhesive fractures due to the weak bonding between the resin and the pristine or sandblasted zirconia surfaces. For the plasma-treated surfaces, 10% of the cohesive/adhesive mixed fractures occurred in the C1, C2, and C4 groups without sandblasting due to the presence of remaining resin debris on the zirconia surface. By contrast, the incidence of mixed fractures in the SB1, SB2, and SB4 groups increased to 40%. The increase in mixed fractures could have originated from the synergistic effect of the mechanical sandblasting and plasma treatment on physical and chemical modifications, respectively. Although the simple evaluation method employed in the present study is not a comprehensive and precise way of

elucidating the fracture behaviour of the specimens, it provides insights to illustrate the relationships between the bond strength and surface characteristics of zirconia with or without surface treatment.

It is worth comparing the difference between sandblasting and plasma treatment in terms of enhancing bond strength. As mentioned above, sandblasting can cause surface defects and phase transformation on the zirconia surface. By contrast, plasma treatment had no such problems. Furthermore, plasma treatment was better than sandblasting in improving the strength of the bonding between the zirconia and composite resin. For example, for the effect of sandblasting on the bond strength, the effect in the SB0 group was 1.7 times that in the C0 group. In the case of the plasma effect, the SB4 group had bond strengths 2.3 times those of the SB0 group, and the C4/C0 strength ratio was 2.8. On the other hand, because the bond strength increased with plasma power, the 400 W plasma treatment (C4 and SB4 groups) resulted in the highest strength of bonding between the zirconia and resin. Out of the plasma powers ranging from 100 to 400 W, 400 W (C4 and SB4 groups) resulted in the highest strength of bonding between the zirconia and resins. Therefore, it is reasonable to speculate that in the range of plasma powers used, plasma treatment was superior to sandblasting treatment in terms of surface morphology, phase composition, and bond strength. Nonetheless, further investigations on the thermocycling and plasma gas effects are needed to elucidate the long-term efficacy and applicability of plasma treatment for zirconia. Although plasma treatment can provide an effective means of improving the surface of existing materials to enhance their physicochemical properties, the commercialization of inexpensive functional equipment is necessary for dental laboratories and clinics. In addition, in order to promote the practical application of plasma in clinical situations, plasma devices (such as hand-held plasma devices) suitable for dental laboratories and clinical practice are still being developed.

## 5. Conclusions

Within the limits of this study, the current results supported the research hypothesis that the shear strength of the bonding of plasma-treated zirconia to resin increased with increasing plasma power. Regardless of sandblasting, the oxygen plasma treatment of zirconia can result in a higher shear strength of the bond with the composite resin than that in the corresponding control group without plasma treatment. In conclusion, oxygen plasma treatment may be a potential way to modify zirconia dental ceramics and improve the strength of the bonding of zirconia to composite resin.

**Author Contributions:** Conceived and designed the experiments, M.Y. and S.-J.D.; Performed the experiments, Y.-H.C.; Analyzed the data, C.-C.Y., M.Y., and S.-J.D.; Wrote the paper, M.Y. and S.-J.D. All authors have read and agreed to the published version of the manuscript.

**Funding:** The authors acknowledge financial support from Chung Shan Medical University (CSMU-INT-107-03) of Taiwan.

**Conflicts of Interest:** The authors declare no conflict of interest.

## References

1. Anusavice, K.; Shen, C.; Ralph Rawls, H. *Phillips' Science of Dental Materials*, 12th ed.; Saunders: Philadelphia, PA, USA, 2013; pp. 30–68.
2. Takeda, T.; Shigami, K.; Shimada, A.; Ohki, K. A study of discoloration of the gingiva by artificial crowns. *Int. J. Prosthodont.* **1996**, *9*, 197–202. [[PubMed](#)]
3. Yan, M.; Kao, C.-T.; Ye, J.-S.; Huang, T.-H.; Ding, S.-J. Effect of preoxidation of titanium on the titanium–ceramic bonding. *Surf. Coat. Technol.* **2007**, *202*, 288–293. [[CrossRef](#)]
4. Buga, C.; Hunyadi, M.; Gácsi, Z.; Hegedűs, C.; Hakl, J.; Schmidt, U.; Ding, S.J.; Csík, A. Calcium silicate layer on titanium fabricated by electrospray deposition. *Mater. Sci. Eng. C* **2019**, *98*, 401–408. [[CrossRef](#)] [[PubMed](#)]
5. Höland, W.; Rheinberger, V.; Apel, E.; Ritzberger, C.; Rothbrust, F.; Kappert, H.; Krumeich, F.; Nesper, R. Future perspectives of biomaterials for dental restoration. *J. Eur. Ceram. Soc.* **2009**, *29*, 1291–1297. [[CrossRef](#)]
6. Yan, M.; Wei, C.-K.; Lin, Y.-Y.; Hu, S.-W.; Ding, S.-J. Impact behavior of three notched all-ceramic restorations after soaking in artificial saliva. *Materials* **2015**, *8*, 4479–4490. [[CrossRef](#)] [[PubMed](#)]

7. Komine, F.; Strub, J.R.; Matsumura, H. Bonding between layering materials and zirconia frameworks. *Jpn. Dent. Sci. Rev.* **2012**, *48*, 153–161. [[CrossRef](#)]
8. Gale, M.; Darvell, B. Thermal cycling procedures for laboratory testing of dental restorations. *J. Dent.* **1999**, *27*, 89–99. [[CrossRef](#)]
9. Vaidyanathan, J.; Vaidyanathan, T.K. Flexural creep deformation and recovery in dental composites. *J. Dent.* **2001**, *29*, 545–551. [[CrossRef](#)]
10. Kobayashi, K.; Komine, F.; Blatz, M.B.; Saito, A.; Koizumi, H.; Matsumura, H.J.Q.I. Influence of priming agents on the short-term bond strength of an indirect composite veneering material to zirconium dioxide ceramic. *Quintessence Int.* **2009**, *40*, 545–551.
11. Komine, F.; Fushiki, R.; Koizuka, M.; Taguchi, K.; Kamio, S.; Matsumura, H. Effect of surface treatment on bond strength between an indirect composite material and a zirconia framework. *J. Oral Sci.* **2012**, *54*, 39–46. [[CrossRef](#)]
12. Han, I.H.; Kang, D.W.; Chung, C.H.; Choe, H.C.; Son, M.K. Effect of various intraoral repair systems on the shear bond strength of composite resin to zirconia. *J. Adv. Prosthodont.* **2013**, *5*, 248–255. [[CrossRef](#)] [[PubMed](#)]
13. Iwasaki, T.; Komine, F.; Fushiki, R.; Kubochi, K.; Shinohara, M.; Matsumura, H. Shear bond strengths of an indirect composite layering material to a tribochemically silica-coated zirconia framework material. *Dent. Mater. J.* **2016**, *35*, 461–469. [[CrossRef](#)] [[PubMed](#)]
14. Sari, F.; Secilmis, A.; Simsek, I.; Ozsevik, S. Shear bond strength of indirect composite material to monolithic zirconia. *J. Adv. Prosthodont.* **2016**, *8*, 267–274. [[CrossRef](#)]
15. Jansen van Vuuren, W.A.; Jansen van Vuuren, L.; Torr, B.; Waddell, J.N. Adhesion between zirconia and indirect composite resin. *Int. J. Adhes. Adhes.* **2016**, *69*, 72–78. [[CrossRef](#)]
16. Lin, T.H.; Chang, H.J.; Chung, K.H. Interfacial strengths of various alloy surface treatment for resin-bonded fixed partial dentures. *J. Prosthet. Dent.* **1990**, *64*, 158–162. [[CrossRef](#)]
17. Mukai, M.; Fukui, H.; Hasegawa, J. Relationship between sandblasting and composite resin-alloy bond strength by a silica coating. *J. Prosthet. Dent.* **1995**, *74*, 151–155. [[CrossRef](#)]
18. Wolfart, M.; Lehmann, F.; Wolfart, S.; Kern, M. Durability of the resin bond strength to zirconia ceramic after using different surface conditioning methods. *Dent. Mater.* **2007**, *23*, 45–50. [[CrossRef](#)]
19. Shimoe, S.; Tanoue, N.; Kusano, K.; Okazaki, M.; Satoda, T. Influence of air-abrasion and subsequent heat treatment on bonding between zirconia framework material and indirect composites. *Dent. Mater. J.* **2012**, *31*, 751–757. [[CrossRef](#)]
20. Zhang, Y.; Lawn, B.R.; Rekow, E.D.; Thompson, V.P. Effect of sandblasting on the long-term performance of dental ceramics. *J. Biomed. Mater. Res. B* **2004**, *71*, 381–386. [[CrossRef](#)]
21. Guazzato, M.; Quach, L.; Albakry, M.; Swain, M.V. Influence of surface and heat treatments on the flexural strength of Y-TZP dental ceramic. *J. Dent.* **2005**, *33*, 9–18. [[CrossRef](#)]
22. Denry, I.L.; Holloway, J.A. Microstructural and crystallographic surface changes after grinding zirconia-based dental ceramics. *J. Biomed. Mater. Res. B* **2006**, *76*, 440–448. [[CrossRef](#)] [[PubMed](#)]
23. Guess, P.C.; Zhang, Y.; Kim, J.W.; Rekow, E.D.; Thompson, V.P. Damage and reliability of Y-TZP after cementation surface treatment. *J. Dent. Res.* **2010**, *89*, 592–596. [[CrossRef](#)] [[PubMed](#)]
24. Okada, M.; Taketa, H.; Torii, Y.; Irie, M.; Matsumoto, T. Optimal sandblasting conditions for conventional-type yttria-stabilized tetragonal zirconia polycrystals. *Dent. Mater.* **2019**, *35*, 169–175. [[CrossRef](#)]
25. Lung, C.Y.K.; Matinlinna, J.P. Aspects of silane coupling agents and surface conditioning in dentistry: An overview. *Dent. Mater.* **2012**, *28*, 467–477. [[CrossRef](#)]
26. Lung, C.Y.K.; Liu, D.; Matinlinna, J.P. Silica coating of zirconia by silicon nitride hydrolysis on adhesion promotion of resin to zirconia. *Mater. Sci. Eng. C* **2015**, *46*, 103–110. [[CrossRef](#)]
27. Scaminaci Russo, D.; Cinelli, F.; Sarti, C.; Giachetti, L.; Scaminaci Russo, D.; Cinelli, F.; Sarti, C.; Giachetti, L. Adhesion to zirconia: A systematic review of current conditioning methods and bonding materials. *Dent. J.* **2019**, *7*, 74. [[CrossRef](#)]
28. El-Shrkawy, Z.R.; El-Hosary, M.M.; Saleh, O.; Mandour, M.H. Effect of different surface treatments on bond strength, surface and microscopic structure of zirconia ceramic. *Future Dent. J.* **2016**, *2*, 41–53. [[CrossRef](#)]
29. Wolter, S.D.; Piascik, J.R.; Stoner, B.R. Characterization of plasma fluorinated zirconia for dental applications by X-ray photoelectron spectroscopy. *Appl. Surf. Sci.* **2011**, *257*, 10177–10182. [[CrossRef](#)]

30. Silva, N.R.; Coelho, P.G.; Valverde, G.B.; Becker, K.; Ihrke, R.; Quade, A.; Thompson, V.P. Surface characterization of Ti and Y-TZP following non-thermal plasma exposure. *J. Biomed. Mater. Res. B* **2011**, *99*, 199–206. [\[CrossRef\]](#)
31. Derand, T.; Molin, M.; Kvam, K. Bond strength of composite luting cement to zirconia ceramic surfaces. *Dent. Mater.* **2005**, *21*, 1158–1162. [\[CrossRef\]](#)
32. Wu, C.C.; Wei, C.K.; Ho, C.C.; Ding, S.J. Enhanced hydrophilicity and biocompatibility of dental zirconia ceramics by oxygen plasma treatment. *Materials* **2015**, *8*, 684–699. [\[CrossRef\]](#)
33. Ito, Y.; Okawa, T.; Fukumoto, T.; Tsurumi, A.; Tatsuta, M.; Fujii, T.; Tanaka, J.; Tanaka, M. Influence of atmospheric pressure low-temperature plasma treatment on the shear bond strength between zirconia and resin cement. *J. Prosthodont. Res.* **2016**, *60*, 289–293. [\[CrossRef\]](#)
34. Liu, T.; Hong, L.; Hottel, T.; Dong, X.; Yu, Q.; Chen, M. Non-thermal plasma enhanced bonding of resin cement to zirconia ceramic. *Clin. Plasma Med.* **2016**, *4*, 50–55. [\[CrossRef\]](#)
35. Park, C.; Park, S.W.; Yun, K.D.; Ji, M.K.; Kim, S.; Yang, Y.P.; Lim, H.P. Effect of plasma treatment and its post process duration on shear bonding strength and antibacterial effect of dental zirconia. *Materials* **2018**, *11*, 2233. [\[CrossRef\]](#)
36. Elias, A.B.; Simao, R.A.; Prado, M.; Cesar, P.F.; Botelho Dos Santos, G.; Moreira da Silva, E. Effect of different times of nonthermal argon plasma treatment on the microtensile bond strength of self-adhesive resin cement to yttria-stabilized tetragonal zirconia polycrystal ceramic. *J. Prosthet. Dent.* **2019**, *121*, 485–491. [\[CrossRef\]](#)
37. Kim, D.S.; Ahn, J.J.; Bae, E.B.; Kim, G.C.; Jeong, C.M.; Huh, J.B.; Lee, S.H. Influence of non-thermal atmospheric pressure plasma treatment on shear bond strength between Y-TZP and self-adhesive resin cement. *Materials* **2019**, *12*, 3321. [\[CrossRef\]](#)
38. ISO/TS 11405. *Dental Materials—Testing of Adhesion to Tooth Structure*; International Organization for Standardization: Geneva, Switzerland, 2015.
39. Cavalcanti, A.N.; Pilecki, P.; Foxton, R.M.; Watson, T.F.; Oliveira, M.T.; Gianinni, M.; Marchi, G.M.; Surgery, L. Evaluation of the surface roughness and morphologic features of Y-TZP ceramics after different surface treatments. *Photomed. Laser Surg.* **2009**, *27*, 473–479. [\[CrossRef\]](#)
40. Lee, P.R.; Ho, C.C.; Hwang, C.S.; Ding, S.J. Improved physicochemical properties and biocompatibility of stainless steel implants by PVA/ZrO<sub>2</sub>-based composite coatings. *Surf. Coat. Technol.* **2014**, *258*, 374–380. [\[CrossRef\]](#)
41. Zhao, G.; Schwartz, Z.; Wieland, M.; Rupp, F.; Geis-Gerstorfer, J.; Cochran, D.L.; Boyan, B.D. High surface energy enhances cell response to titanium substrate microstructure. *J. Biomed. Mater. Res. A* **2005**, *74*, 49–58. [\[CrossRef\]](#)
42. Valverde, G.B.; Coelho, P.G.; Janal, M.N.; Lorenzoni, F.C.; Carvalho, R.M.; Thompson, V.P.; Weltemann, K.-D.; Silva, N.R.F.A. Surface characterisation and bonding of Y-TZP following non-thermal plasma treatment. *J. Dent.* **2013**, *41*, 51–59. [\[CrossRef\]](#)

